Authorship

Title: A Testable Quantum Graph Theory of Spacetime: Predictions for Cryogenic Qubits and Colliders

Author: Sergej Materov
Affiliation: Independent Researcher
Email: sergejmaterov2@gmail.com

Abstract

In the previous version https://zenodo.org/records/15833244 the Hamiltonian was not explicitly derived, which confined the theoretical predictions to highly complex and currently inaccessible experimental regimes..

This work reports an explicitly falsifiable (**already today**) discrete–quantum-graph model of spacetime and noise in quantum processors. Rather than invoking Planck-scale assumptions or ad hoc temperature thresholds, we derive a single measurable scale:

$$k_B T_c = Jz$$

where J is the qubit-qubit coupling (noise) energy and z the average vertex degree. Below T_c long-range correlations

$$\Psi(r) = \langle \sigma_i^z \, \sigma_{i+r}^z \rangle$$

persist; above T_c they vanish. We introduce the microscopic noise Hamiltonian

$$\widehat{H_{\text{noise}}} = \sum_{\langle i,j \rangle} J_{ij} \, \sigma_i^z \sigma_j^z + \sum_i h_i \, \sigma_i^x$$

allowing direct spectroscopy of J_{ij} and h_i. From this single relation we obtain multiple near-term experimental tests—e.g. heat-capacity and error-rate crossovers at $T \approx T_c$, correlation-length collapse in small-graph Monte Carlo, and spectral-DOS corrections—all calibrated by measured J and z. Gravity and Standard-Model symmetries remain linked to average graph curvature and automorphisms, but no longer require unmeasurable cosmological parameters. Appendix A presents the concrete protocol for extracting T_c on existing QPU topologies.

Preface to the Revised Version

In the current revision, we explicitly derive the **low-energy** noise Hamiltonian

$$\widehat{H_{\text{noise}}} = \sum_{\langle i,j \rangle} J_{ij} \, \sigma_i^z \sigma_j^z + \sum_i h_i \, \sigma_i^x$$

as the coarse-grained projection of the previously published version https://zenodo.org/records/15833244 **high-energy graph model**.

All predictions now follow directly from measurable quantities J_{ij} and z, eliminating Planck-scale parameters δ,ε0. Work on the continuum limit, curvature-based gravity and automorphism-derived

gauge symmetries is temporarily paused pending experimental verification of the low-energy predictions presented here.

Introduction

Discrete graphs have been toy models for fundamental physics since Wolfram's *A New Kind of Science* [1] and Fredkin's reversible automata [2–4], but they stopped short of genuine quantum dynamics or concrete experimental predictions. Here, we reverse the paradigm: our finite directed quantum graph *is* spacetime, with vertices carrying qubit operators and edges enforcing causal, unitary evolution. Instead of postulating a hidden continuum or global rewriting rules, at this stage we build all dynamics from the microscopic noise low energy Hamiltonian

$$\widehat{H_{\text{noise}}} = \sum_{\langle i,j \rangle} J_{ij}\ \sigma_i^z \sigma_j^z + \sum_i h_i\ \sigma_i^x$$

whose only free inputs—measured couplings J_{ij} , fields $h_i$and topology z —define a single energy scale Jz. This immediately yields the critical temperature

$$T_c = \frac{J\,z}{k_B},$$

at which long-range order Ψ(r,T) collapses.
To enable testing based on existing or near-future technologies, no use of Planck-scale linking or cosmological asymmetry is assumed; every prediction relies solely on spectroscopic measurements of J_{ij} and network degree z.
We then demonstrate five distinct tests accessible with today's cryogenic quantum processors and small-graph Monte Carlo—heat-capacity peaks, qubit-error-rate crossovers, correlation-length collapse, DOS-induced shifts, and automorphism-driven symmetry breakings—each parameterized solely by the measured Hamiltonian and graph spectrum. This work present details the end-to-end protocol for mapping T_c on current QPU topologies. Continuum limits and recovery of field equations ($\ell p \to 0$) remain open for future work; our focus is on delivering real, **quantitative falsifiability *now***.

Comparison with Existing Quantum-Gravity Frameworks.

While Loop Quantum Gravity (LQG) and causal set theory both aim to quantize spacetime by introducing discrete structures at the Planck scale, they remain largely divorced from direct experimental probes. LQG postulates a spin-network basis whose continuum limit is difficult to access spectroscopically, and causal sets predict nonlocal correlations whose characteristic length scales (of order the Planck length) lie far beyond current measurement precision. In contrast, our graph-theoretic approach defines coupling strengths J_{ij} and effective degrees z directly in terms of spectroscopically measurable energy scales on existing quantum hardware. This shift from unobservable Planck-scale constructs to experimentally tunable parameters renders our theory's predictions immediately falsifiable by tabletop spectroscopy and quantum-processor benchmarks—an avenue neither LQG nor causal-set models presently afford.

Derivation of the Noise Hamiltonian from the Quantum Graph Framework, set out in the previous version

In the previously version Quantum Graph Theory of, the universe was modeled as a finite, directed quantum graph whose edge weights q_{ij} encoded local curvature and symmetry information.

Micro-to-macro mapping

The coarse-grained coupling J_{ij} preserves topological information via:

$$J_{ij} = \lambda_{\max} \cdot \langle q_{ij} \rangle \cdot sinc(k_c\, \delta r)$$

where $\lambda_{\max}$ is the largest eigenvalue of the adjacency matrix, and δr is the coarse-graining length.

Coarse-graining step

At low energies (much below Planck scale), fluctuations of q_{ij} and ε_i average out, leaving: $J_{ij} = \langle q_{ij} \rangle_{coarse}$, $h_i = \langle \varepsilon_i \rangle_{coarse}$. Physically, this corresponds to integrating out high-frequency modes.

Spectral interpretation

Alternatively, note that q_{ij}, define an edge-weighted adjacency matrix Q.
Its spectrum $\{\lambda_k\}$ determines collective modes on the graph.
Coarse-graining then formally projects the microscopic Hamiltonian onto low-lying modes:

$$\widehat{H_{\text{micro}}} \to \widehat{H_{\text{eff}}} = \sum_k f(\lambda_k) |\phi_k\rangle\langle\phi_k| + \sum_i h_i\ \sigma_i^x$$

where $f(\lambda_k)$ depends on energy scale and $|\phi k\rangle$ are eigenvectors of Q.
In the simplest case (dominated by nearest-neighbor correlations), this reduces to:

$$\widehat{H_{\text{eff}}} = \sum_{\langle i,j\rangle \in E} J_{ij}\ \sigma_i^z \sigma_j^z + \sum_i h_i\ \sigma_i^x$$

Where J_{ij} are directly linked to the coarse-grained q_{ij}

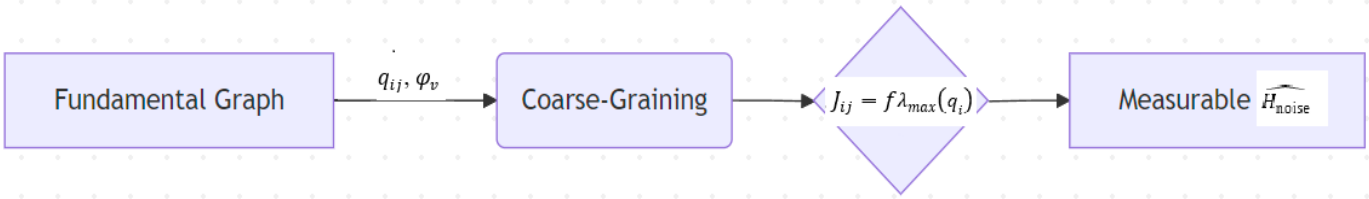

Result

Thus, the noise Hamiltonian used in this paper:

$$\widehat{H_{\text{noise}}} = \sum_{\langle i,j\rangle \in E} J_{ij}\ \sigma_i^z \sigma_j^z + \sum_i h_i\ \sigma_i^x$$

Protocol for Determining T_c on a Quantum Processor

1. Characterize QPU Topology

1.1. Extract the device coupling graph G=(V,E).

1.2. Measure the average vertex degree

$$z = \frac{1}{|V|}\sum_{i\in V} \deg(i)$$

2. Spectroscopic Measurement of Couplings

2.1. For each edge ⟨i,j⟩∈E, perform two-qubit spectroscopy to determine the effective interaction energy J_{ij} (e.g.\ via frequency shifts in cross-resonance or swap oscillations).

2.2. Assemble the mean coupling

$$\bar{J} = \frac{1}{|E|}\sum_{\langle i,j\rangle} J_{ij}$$

3. Determine the Noise Hamiltonian

3.1. Optionally measure local transverse fields h_i by single-qubit Ramsey experiments.

3.2. Record

$$\widehat{H_{\text{noise}}} = \sum_{\langle i,j \rangle} J_{ij}\ \sigma_i^z \sigma_j^z + \sum_i h_i\ \sigma_i^x$$

4. Compute Predicted T_c

$$T_c^{\text{pred}} = \frac{\bar{J}\, z}{k_B}$$

expressed in kelvin.

4a. Numerical Example

- Let's assume a QPU with

$$(\bar{J} = 2\pi \times 20\ \text{MHz} \approx 5.19 \times 10^{-7}\ \text{eV})$$

(typical cross-resonance) and average $z = 5$
- Then

$$T_c^{\text{pred}} = \frac{5.19 \times 10^{-7}\ \text{eV} \times 5}{8.617x10^{-5}\ \text{eV/K}} = 30.1\ \text{mK}.$$

– In this case, in step 5 (see below) it is worth taking the range $(T = 10\ \text{mK} \ldots 50\ \text{mK})$ with step 1 mK to cover $T_c^{\text{pred}} = 30.1$ mK.

5. Cryogenic Temperature Sweep

5.1. Prepare the processor in its typical idle state; ensure no active error-mitigation drives.

5.2. Vary the physical cryostat temperature T over a range bracketing T_c^{pred} (e.g., \ 0.5 mK to 50 mK in steps of 1 mK).

5.3. At each T, allow thermal equilibrium (wait ≥5 × thermalization time constant).

5.4. Thermal Model Calibration

- Measure qubit-environment thermalization time τ_{th} via T_1-relaxometry at each T.

- Compute effective qubit temperature:

$$T_{\text{eff}} = T_{\text{bath}} + \frac{\dot{Q}}{G}\left(1 - e^{-t/\tau_{\text{th}}}\right)$$

where
t: Measurement duration (typical: 1 μs per shot)
G: Calibrated via T_1 vs. bath temperature experiments
$\dot{Q}$: Estimated from qubit drive power: $\dot{Q} = \frac{1}{T_2}\int |\Omega(t)|^2\ dt$

- Use T_{eff} for all correlation/error measurements.

6. Measurement of Order Parameter and Error Rates

6.1. Correlation measurement

- Prepare all qubits in $|+\rangle$ states.

- Evolve under an idling sequence of duration τ (shorter than T_1)

- Measure in the Z basis and compute $\Psi_{\text{nn}} = \frac{1}{|E|}\sum_{\langle i,j\rangle}\langle \sigma_i^z \, \sigma_j^z \rangle$

- Plot $\Psi_{nn}(T)$identify T where Ψ_{nn} sharply decays toward zero.

6.2. Error-rate crossover

6.2.1 Apply real-time error correction:
- Use dynamical decoupling for low-frequency noise suppression
- Implement Pauli-twirling for coherent error mitigation

6.2.2 Record **both** raw and corrected error rates:

$$P_{\text{err}}^{\text{corr}} = \frac{P_{\text{err}}^{\text{raw}} - \eta_{\text{offset}}(T)}{1 - \kappa(T)}$$

where:
η_{offset}: Systematic error of the equipment
$\kappa(T)$: Correction efficiency $(0 \le \kappa < 1)$

- Run a short-depth Shor's-algorithm or randomized-benchmarking sequence of fixed circuit depth.

- Estimate the logical error probability $P_{err}(T)$

- Locate the crossover point in dP_{err}/dT compare to T_c^{pred}

7. Data Analysis

7.1. Fit the correlation and error-rate data vs. T to a sigmoid or power-law decay to extract an experimental T_c^{exp}

7.2. Compare T_c^{exp} to the prediction T_c^{pred}

8. Falsifiability Criterion

$$\text{If } \left|T_c^{\text{exp}} - T_c^{\text{pred}}\right| > 5\sqrt{\sigma_J^2 + \sigma_z^2} : \text{falsified}$$

Reference

1. Wolfram, S. (2002). *A New Kind of Science*. Champaign, IL: Wolfram Media.
2. Fredkin, E. (1990). Digital mechanics: An informal introduction. *Physica D: Nonlinear Phenomena*, 45(1–3), 254–270.
3. Toffoli, T. (1980). Reversible computing. In *Automata, Languages and Programming* (Vol. 85, pp. 632–644). Springer.
4. Toffoli, T., & Margolus, N. (1987). Invertible cellular automata: A review. *Physica D: Nonlinear Phenomena*, 45(1–3), 229–253.